Proc. Int. Symposium on Neutron Optics and Related Research Facilities, Kumatori, 1996
J. Phys. Soc. Jpn. 65 (1996) Suppl. A pp. 241-244

Bent Crystal Analyzer in Fully Asymmetric Diffraction Geometry for Neutron Scattering Instrumentation

Petr LUKÁŠ, Zdeněk KOUŘIL, Pavel MIKULA, Jan ŠAROUN, Pavel STRUNZ, Miroslav VRÁNA and *Volker WAGNER

Nuclear Physics Institute, 250 68 Řež near Prague, Czech Republic
**Physikalisch-Technische Bundesanstalt, 38116 Braunschweig, Germany*

(Received 6 February 1996; accepted 18 April 1996)

Silicon bent perfect crystals in fully asymmetric diffraction (FAD) geometry in combination with a linear position sensitive detector are used for analysis of diffracted neutron beams. Three original neutron diffraction arrangements exploiting this neutron-optical element are reported: a double-crystal SANS instrument and two high-resolution diffractometers for measurement of strains in polycrystalline materials.

KEYWORDS: bent crystals, asymmetric diffraction geometry, SANS, strains

1. Introduction

Investigations of Bragg diffraction optics with bent perfect crystals in NPI Řež have resulted in many useful applications.[1,2] A lot of attention has been paid to testing various designs of neutron monochromators based on bent perfect crystals of silicon and germanium, respectively, such as horizontally and vertically focusing monochromators,[3] monochromators of sandwich type[4], etc. Besides monochromators, a neutron-optical device consisting of the elastically bent perfect Si crystal in fully asymmetric diffraction (FAD) geometry in combination with a position sensitive detector (PSD) has been found very effective in different experimental diffraction arrangements. This device was designed to avoid a conventional step-by-step analysis performed by a rotation of an analyzer-crystal in symmetric Bragg reflection geometry equipped with a neutron counter. The analyzer in FAD geometry makes it possible to transform the (angle, wavelength) correlation of neutrons to (space, wavelength) correlation, and analyzed neutron spectra can be thus collected simultaneously by a linear PSD. Diffraction properties of this arrangement, especially focusing effects, were simulated by Monte Carlo method and experimentally studied as well, e.g. in ref. 5,6. Three experimental arrangements successfully employing such analyzers --- a double-bent-crystal (DBC) diffractometer for SANS investigation in medium Q region[7] and two experimental arrangements for high - resolution strain / stress measurements --- are reported in this paper. Triple-axis diffractometer[8] using focusing effects in real and momentum space enables a determination of macro- and micro-strains of the order of 10^{-4}. Even higher sensitivity to changes in lattice spacing ($\Delta d/d$ down to 10^{-5}) can be reached in energy-dispersive neutron transmission diffraction geometry.[9]

2. Neutron-optical properties of the analyzer in FAD geometry with PSD

The principal sketch of the analyzer is shown in Fig.1. Bent perfect crystals usually produce much sharper correlation between phase space variables than flat mosaic crystals. Therefore, both momentum and real space focusing effects have to be accounted for if we want to find a precise relation between the spatial coordinate x_D of the PSD and the corresponding momentum and/or energy transfer. For this purpose we can express Bragg condition in a differential form as

$$0 = \gamma_i - \eta_i + \frac{\Delta k}{k} \tan\theta_i + \frac{x_i}{R_i}, \quad (1)$$

where γ_i is an angular deviation of a neutron trajectory from the central beam, x_i a spatial coordinate of the place in the crystal where the Bragg condition is fulfilled, η_i the crystal inclination angle, and R_i its bending radius. The index i=M,A,S denotes the monochromator, analyzer, and sample (in the case of diffraction experiments). For elastic and isotropic scattering, usually in the assumed case of powder diffraction or SANS, only the magnitude of the momentum transfer Q is of our interest. Let us define focusing parameters

$$\xi_M = 1 - \frac{L_{MS}}{2f_M}, \quad \xi_A = 1 - \frac{L_{AD}}{2f_A},$$
$$\xi_{A1} = 1 - \frac{L_{AD}}{f_A}, \quad (2)$$

where L_{MS} and L_{AD} are the monochromator-sample and analyzer-detector distances, respectively, and

$$f_M = \frac{1}{2} R_M \sin\theta_M, \; f_A = \frac{1}{2} R_A \sin(2\theta_A) \quad (3)$$

are the focal lengths. The relation between Q and x_D can

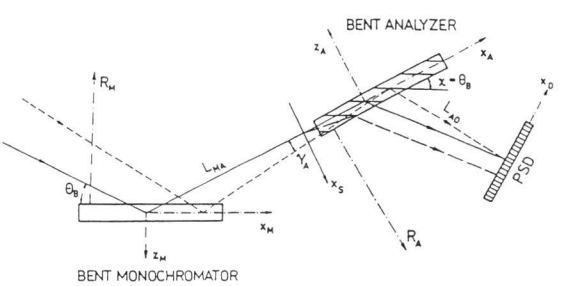

Fig.1. Schematic sketch of the analyzer in FAD geometry.

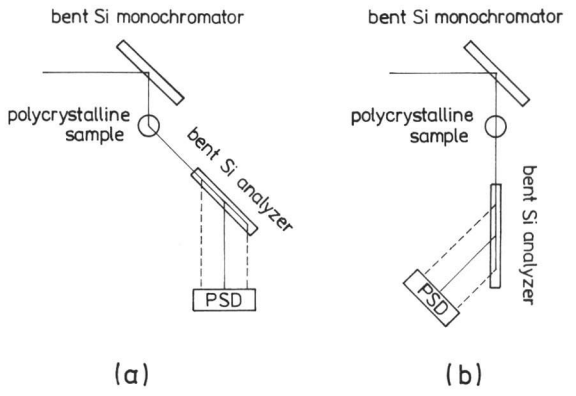

Fig.2. Experimental settings. (a) High-resolution strain diffractometer. (b) Energy dispersive transmission geometry.

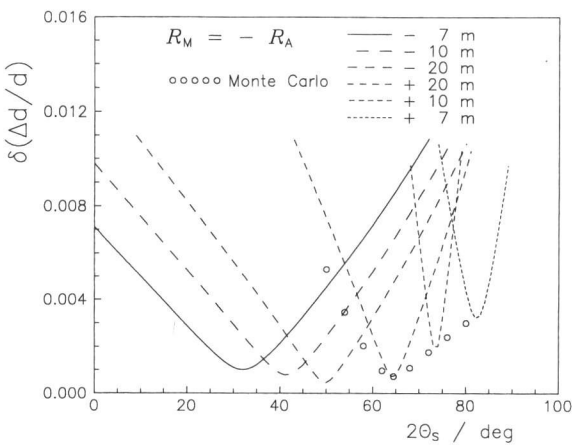

Fig.3. Instrumental resolution of strain diffractometer calculated for different R_A and R_M.

be derived from simple geometrical considerations and from the Bragg condition (1) for the monochromator and analyzer in the following form

$$\frac{1}{2} f_A^{-1} x_D = -\xi_A \frac{Q}{k} + \frac{\Delta k}{k}\left(\frac{\xi_A}{\xi_M}\tan\theta_M + \xi_{A1}\tan\theta_A\right). \quad (4)$$

This equation can be applied to all three types of experiments considered in this paper.

2.1 Small-angle scattering, (1,-1) setting

In this case $\theta_M = -\theta_A$ and the second term on the right-hand side of eq.(4) reduces to

$$\frac{\Delta k}{k}\tan\theta_M \frac{1}{2}\left(\frac{L_{AD}}{f_A} + \frac{L_{MS}}{f_M}\right)\xi_M , \quad (5)$$

determining the Q-resolution. This term can be set to zero by choosing bending radii properly. The resolution is then given by other contributions not included in eq.(4), resulting e.g. from the monochromator thickness, sample dimensions, or detector resolution. For more details see ref. 5.

2.2 High resolution diffraction, (1,-1,1) setting

In the case when a powder or polycrystalline sample is put between the monochromator and the analyzer (Fig.2a), we can substitute Q/k in eq.(4) by the angular deviation η_S corresponding to an individual grain,

$$\frac{Q}{k} = 2\eta_S = 2\left(\frac{\Delta d}{d} - \frac{\Delta k}{k}\right)\tan\theta_S . \quad (6)$$

We arrive then at the following expression for the relative change of the lattice spacing,

$$\frac{\Delta d}{d} = \frac{1}{4}(f_A\xi_A)^{-1}\cot\theta_S x_D \quad (7)$$

and the corresponding resolution,

$$\delta\left(\frac{\Delta d}{d}\right) = \frac{1}{2}\delta\left(\frac{\Delta k}{k}\right)\cot\theta_S\left[\xi_M^{-1}\tan\theta_M + \frac{\xi_{A1}}{\xi_A}\tan\theta_A + 2\tan\theta_S\right]. \quad (8)$$

By proper tuning crystal curvatures, the expression in the brackets can be minimized and a sharp minimum in resolution can be achieved for a given θ_S. This effect is documented in Fig.3 where the resolutions for different crystal curvatures and θ_S are plotted; however, a more complex formula including also other contributions[5] to the resolution was used. These contributions do not affect the positions of the minima essentially.

2.3 Transmission spectrum, (1, 1) setting

In a dispersive setting (Fig.2b) with θ_M and θ_A of the same sign, the energy distribution of neutrons can be also analyzed as follows from eq.(4). This possibility was utilized in precise measurements of Bragg diffraction edges in transmission spectra of polycrystals.

3. Neutron Diffraction Instrumentation

In all instruments employing bent perfect crystals, we are using four-point bending devices with crystal slabs of standard dimensions 40x200 mm^2 (height x length) and of a thickness ranging from 3 to 7 mm. Crystal slabs of different crystallographic orientations are available, e.g. (110), (111) or (112) lattice planes parallel to the main surface of the crystal slab. The bending devices enable a reproducible adjustment of the bending radii from infinity (flat crystal) to 5 m (thinner crystals). He^3 1-dimensional PSD with an active window of 200x40 mm^2 are used. The spatial resolution of the PSD is about 1mm.

3.1 Double crystal SANS diffractometer

The DBC diffractometer equipped with the bent perfect Si crystals both set in the symmetric Bragg geometry has been used successfully for medium resolution SANS experiments at NPI since 1983. The angular resolution of the SANS diffractometer as well as its luminosity can be tuned easily by the bending of both crystals according to the tasks of a particular experiment. The instrument has operated in the Q-range from 2x10^{-4} to 2x10^{-2} Å^{-1} overlapping a Q-gap existing between conventional pin-hole instruments (usually Q>10^{-2} Å^{-1}) and high-resolution Bonse-Hart cameras (Q<10^{-3} Å^{-1}). The fully asymmetric analyzer with the PSD was designed in 1987 to improve the existing experimental setup. After methodological tests, the instrument was realized at the 8th beam of the LVR-15 reactor in Řež[7] and later on, in HMI Berlin (instrument V12[10]). The schematic sketch of the DBC instrument is shown in Fig.1. The neutron wavelength is λ=2.1 Å, the (111) reflections are employed in both monochromator and analyzer. The callibration function $Q(x_D)$ is determined experimentally when the analyzer is rotated with equidistant angular steps and the shift of diffraction profile center along the PSD is recorded. This function was found

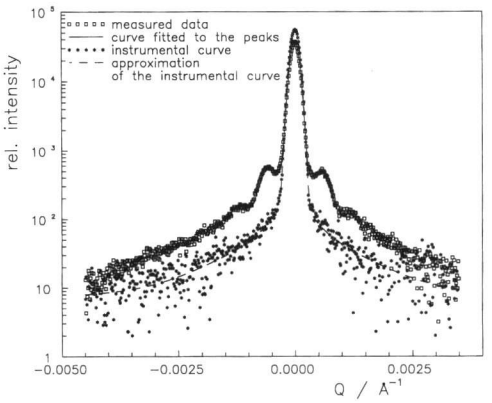

Fig.4. SANS from cuboidal γ′ precipitates in the single crystal Ni based super-alloy.

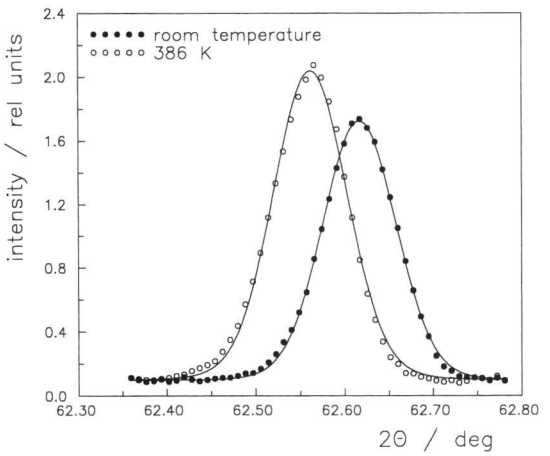

Fig.5. Fe(110) diffraction profiles at two different temperatures.

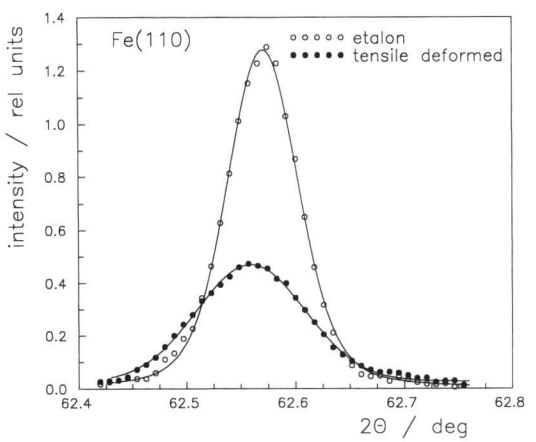

Fig.6. Broadening of Fe(110) profile with a tensile deformation.

to be the exact linear function[7] as predicted by eqs. (4,5). Taking into account the peak intensities, the correction function for intensity attenuation along the analyzer length can be also obtained from this callibration. The attenuation depending on x_D is a relatively small correction, usually within 20%. The useful beam cross section is typically of about 5x40 mm^2 being limited by the anlyzer-crystal dimensions (7x40x200 mm^3). As a practical demonstration of a successful exploitation of the medium resolution DBC camera, we are presenting results of a recent SANS experiment on Ni-based single crystal superalloy (Fig.4). This measurement enabled a determination of average distance between ordered cuboidal γ′ precipitates which was calculated from the distance of the interparticle interference maxima. Due to the instrumental resolution, this effect could be observed only at few existing SANS collimator systems.

3.2 High-resolution strain/stress diffractometer

In the last decade, much neutron diffraction work has been dedicated to determination of internal strains in polycrystalline materials.[11] Both elastic and plastic strains are commonly investigated. The elastic strain $\varepsilon = \Delta d/d$ is deduced from small shifts of a diffraction peak from its position in unstrained sample. Peak shifts are then converted to strains by differentiating Bragg's equation to give $\varepsilon = -\cot\theta \cdot \Delta\theta$. The plastic strain, related to stress fields of microstructural defects, results in broadening of the diffraction profile. Various profile analysis procedures[12] are applied in this case to quantify microstrains and separate them from grain size contribution to peak broadening. The original triple-axis setup equipped with a bent Si single crystal monochromator and analyzer both in symmetric Bragg geometry for investigation of strains was realized at NPI in 1991 and has operated in a user regime since that time.[13] The diffractometer takes advantage of the focusing both in real and momentum space, and yields resolution and luminosity comparable to those of the best powder diffractometers. However, it should be pointed out that such excellent properties of the device may be reached only in a limited Q-range in the vicinity of the selected Bragg reflection with respect to which all focusing conditions are optimized (Fig.3). The instrument is usually tuned to $d = 2$ Å, where a strong reflection can be usually found for most metals, e.g. Fe(110), Ni(111), and Cu(111). Recently, the asymmetric analyzer has been tested at this instrument to accelerate data collection. The scheme of the arrangement is in Fig.2a. The inspected sample volume is determined by two fixed Cd slits (1 to 2 mm width, usually) in the incident and diffracted beam, respectively. Using $\lambda = 2.2$ Å, the 3-axis combination of Si(111)/Fe(110)/Si(220) was examined for the asymmetric analyzer. The instrumental resolution estimated from the diffraction profile of a well annealed Fe etalon (FWHM($\Delta d/d$)=1.4x10^{-3}) was even better than with the convential symmetric analyzer (FWHM($\Delta d/d$)=2x10^{-3}). Figure 5 demonstrates simulation of the macrostrain by heating an α-Fe sample to a temperature about 386 K. Using the PSD, the diffraction profile (with a sufficient count rate necessary for determination of $\Delta d/d$ with an accuracy of about 10^{-4}) for a 0.1 cm^3 gauge volume can be taken at a medium power reactor in several minutes. The broadening of the Fe(110) diffraction profile brought about by a tensile plastic deformation is demonstrated in Fig.6.

3.3 Energy-dispersive transmission diffraction

Energy-dispersive transmission diffraction techniques are usually used at pulsed neutron sources,[14] and the Bragg diffraction edges at $2\theta_S = 180^\circ$ are examined in TOF regime. The modified technique for steady state reactors has been proposed and tested in our laboratory for strain/stress experiments.[9] In comparison with TOF techniques, the only one Bragg diffraction edge is investigated in this case; however, this disadvantage is eliminated by considerably high resolution. The scheme of

the double-crystal experimental arrangement is displayed in Fig.2b. The reflection combination Si(220)/Fe(321)/Si(400) for λ = 1.53 Å was tested. The instrumental resolution was appreciated by the width of the (321) edge of a well-annealed α-Fe etalon sample being about 8×10^{-4} ($\Delta d/d$), that gives a sensitivity down to 10^{-5} in determination of strains. The extremely high sensitivity to small lattice distortions was demonstrated in the measurement of the shift of the Fe(321) Bragg edge from the Fe etalon sample with increasing temperatures at 7°C and 13°C, respectively (Fig.7). This experimental arrangement can be used obviously to investigate plastic deformation of materials in its early stage, in analogy with the classical diffraction profile analysis. Although the shape of the Bragg edge is determined dominantly by $\Delta d/d$ distribution, the simple conversion of the problem to existing methods of profile analysis is not obviously possible and a proper theory of profile analysis of diffraction edges be formulated. The broadening of the diffraction edge with increasing microstrain was demonstrated experimentally on the set of conventional construction carbon steel deformed plastically up to 20%. Some examples of broadened edge profiles are in Fig.8, and the results are summarized in Fig. 9, where the widths of the observed edges are plotted against the degree of deformation. The FWHM in Fig.9 is the FWHM of a Gaussian function as the first derivative of an error function, which was used for fitting the shape of diffraction edges.

4. Conclusion

Due to its luminosity and resolution, the reported asymmetric analyzer has been found to be a very effective construction element in various neutron diffraction arrangements. Generally, much faster data acquisition is achieved in comparison with the conventional analyzer in symmetric geometry, typically with a factor of 50-100. It enables one to perform high-resolution experiments (such as strain measurements) even at medium power reactors for a reasonable sample volume and counting time. The results discussed in section 3.3 were obtained at a 1 MW reactor (PTB Braunschweig).

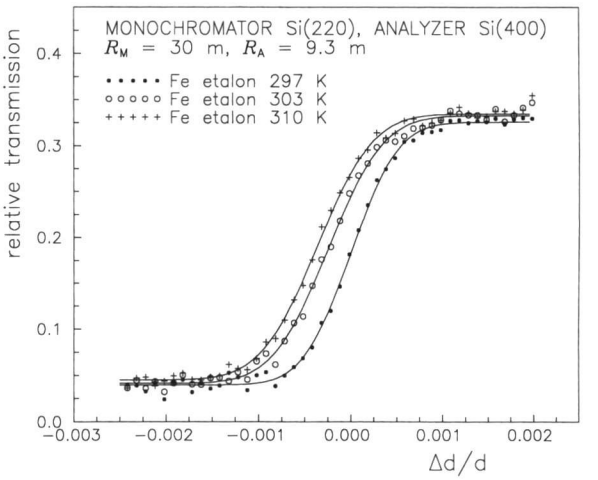

Fig.7. Shift of the Fe(321) Bragg diffraction edge with heating the sample.

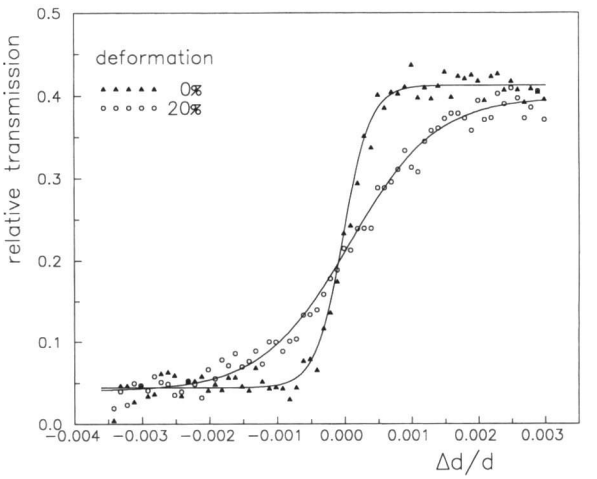

Fig.8. Broadening of the Fe(321) Bragg diffraction edge with 20% tensile deformation of the sample.

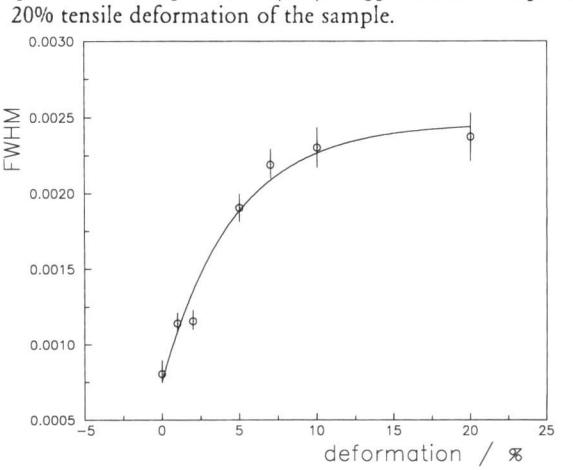

Fig.9. FWHM of Fe(321) Bragg diffraction edge vs. tensile deformation.

1) P.Mikula, J.Kulda, P.Lukáš, M.Vrána, V.Wagner, *Nucl. Instr. and Meth. in Phys. Res.* A338 (1994) 18.
2) N.Nimura et al., *Physica* B 213&214 (1995) 786.
3) J.Kulda and J. Šaroun, *preprint ILL* 95KU5082, ILL Grenoble 1995, *Nucl. Instr. and Meth.* A, submitted.
4) P.Mikula, P.Lukáš, J.Šaroun , V.Wagner and J.Kulda, *Physica* B 213&214 (1995) 922.
5) J.Šaroun et al., *J.Appl.Cryst.* 27, (1994), 80-88.
6) J.Šaroun et al., *J. Phys. IV, Colloque* C8, 3 (1993) 439.
7) P.Lukáš, P.Mikula, J.Šaroun, P.Strunz, *Nucl. Instr. and Meth. in Phys. Res.* A338 (1994) 111.
8) M.Vrána, P.Lukáš, P.Mikula and J.Kulda, *Nucl. Instr. and Meth. in Phys. Res.* A338 (1994) 124.
9) P.Mikula et al., *Physica* B 213&214 (1995) 845.
10) A.Hempel, F.Eichhorn, *BENSC Experimental Reports 1994*, HMI Berlin, 1994, p.350.
11) M.T.Hutchings and A.D.Krawitz (eds.) *Measurement of Residual and Applied Stress Using Neutron Diffraction*, NATO ASI Series, Applied Sciences 26 (Kluwer Acad. Publ., 1992).
12) D. Balzar, *J. Res. Natl. Inst. Stand. Technol.* 98 (1993) 321.
13) K.Macek et al., *Mat. Sci. Eng.* (1996), in print.
14) H.G.Priesmeyer, J.Larsen and K.Meggers, *J. Neutron Research* 2 (1994) 31.